JCI The Journal of Clinical Investigation

Intestinal epithelial vitamin D receptor signaling inhibits experimental colitis

Weicheng Liu, … , Stephen B. Hanauer, Yan Chun Li

J Clin Invest. 2013;123(9):3983-3996. https://doi.org/10.1172/JCI65842.

Research Article **Gastroenterology**

The inhibitory effects of vitamin D on colitis have been previously documented. Global vitamin D receptor (VDR) deletion exaggerates colitis, but the relative anticolitic contribution of epithelial and nonepithelial VDR signaling is unknown. Here, we showed that colonic epithelial VDR expression was substantially reduced in patients with Crohn's disease or ulcerative colitis. Moreover, targeted expression of human VDR (hVDR) in intestinal epithelial cells (IECs) protected mice from developing colitis. In experimental colitis models induced by 2,4,6-trinitrobenzenesulfonic acid, dextran sulfate sodium, or $CD4^+CD45RB^{hi}$ T cell transfer, transgenic mice expressing hVDR in IECs were highly resistant to colitis, as manifested by marked reductions in clinical colitis scores, colonic histological damage, and colonic inflammation compared with WT mice. Reconstitution of *Vdr*-deficient IECs with the *hVDR* transgene completely rescued *Vdr*-null mice from severe colitis and death, even though the mice still maintained a hyperresponsive *Vdr*-deficient immune system. Mechanistically, VDR signaling attenuated PUMA induction in IECs by blocking NF-κB activation, leading to a reduction in IEC apoptosis. Together, these results demonstrate that gut epithelial VDR signaling inhibits colitis by protecting the mucosal epithelial barrier, and this anticolitic activity is independent of nonepithelial immune VDR actions.

Intestinal epithelial vitamin D receptor signaling inhibits experimental colitis

Weicheng Liu,[1] Yunzi Chen,[1,2] Maya Aharoni Golan,[1] Maria L. Annunziata,[1] Jie Du,[2] Urszula Dougherty,[1] Juan Kong,[1,2] Mark Musch,[1,3] Yong Huang,[1] Joel Pekow,[1] Changqing Zheng,[4] Marc Bissonnette,[1,3] Stephen B. Hanauer,[1] and Yan Chun Li[1,2,3]

[1]Department of Medicine, The University of Chicago, Chicago, Illinois, USA. [2]Laboratory of Metabolic Disease Research and Drug Development, China Medical University, Shenyang, Liaoning, China. [3]Committee on Molecular Metabolism and Nutrition, Division of Biological Sciences, The University of Chicago, Chicago, Illinois, USA. [4]Division of Gastroenterology, Shengjing Hospital, China Medical University, Shenyang, Liaoning, China.

The inhibitory effects of vitamin D on colitis have been previously documented. Global vitamin D receptor (VDR) deletion exaggerates colitis, but the relative anticolitic contribution of epithelial and nonepithelial VDR signaling is unknown. Here, we showed that colonic epithelial VDR expression was substantially reduced in patients with Crohn's disease or ulcerative colitis. Moreover, targeted expression of human VDR (hVDR) in intestinal epithelial cells (IECs) protected mice from developing colitis. In experimental colitis models induced by 2,4,6-trinitrobenzenesulfonic acid, dextran sulfate sodium, or $CD4^+CD45RB^{hi}$ T cell transfer, transgenic mice expressing hVDR in IECs were highly resistant to colitis, as manifested by marked reductions in clinical colitis scores, colonic histological damage, and colonic inflammation compared with WT mice. Reconstitution of *Vdr*-deficient IECs with the *hVDR* transgene completely rescued *Vdr*-null mice from severe colitis and death, even though the mice still maintained a hyperresponsive *Vdr*-deficient immune system. Mechanistically, VDR signaling attenuated PUMA induction in IECs by blocking NF-κB activation, leading to a reduction in IEC apoptosis. Together, these results demonstrate that gut epithelial VDR signaling inhibits colitis by protecting the mucosal epithelial barrier, and this anticolitic activity is independent of nonepithelial immune VDR actions.

Introduction

Ulcerative colitis (UC) and Crohn's disease (CD) are major chronic inflammatory bowel diseases (IBDs) in humans. Although the etiology and pathogenesis of IBD remain uncertain, it is believed that derangements in the complex interplay among genetic, environmental, microbial, and immune factors contribute to these disorders (1). Impaired gut mucosal barrier function is thought to be a significant pathogenic factor leading to intestinal hyperpermeability in IBD (2). The epithelial barrier consists of a monolayer of epithelial cells with intercellular junctions between adjacent cells that seal the paracellular space and regulate barrier permeability (3). This barrier prevents harmful solutes, microorganisms, toxins, and luminal antigens from entering the body (4). Compromised barrier function results in the invasion of luminal antigens and bacteria into the lamina propria, which triggers an immune response that leads to chronic colonic inflammation (5).

Aberrant apoptosis of intestinal epithelia cells (IECs) is thought to be a major pathogenic mechanism leading to increased mucosal permeability and colonic inflammation. Increased IEC apoptosis has been reported in patients with UC and CD (6–8) as well as in murine models of colitis (9, 10). Excess IEC apoptosis causes focal disruption of the mucosal barrier, leading to invasion of luminal antigens and bacteria, and proinflammatory cytokines induced in this process can cause more IEC apoptosis. This vicious cycle of events eventually results in clinical symptoms of IBD. Indeed, TNF-α and IFN-γ, two cytokines critical to IBD pathogenesis, induce IEC apoptosis (11). Recent studies demonstrated that p53-upregulated modulator of apoptosis (PUMA) is a key mediator of IEC apoptosis in IBD (12). PUMA is a BH3 domain proapoptotic BCL2 family member that interacts with antiapoptotic BCL2 family members to activate proapoptotic BAX and BAK and trigger mitochondrial dysfunction. This results in the release of several apoptogenic mitochondrial proteins, such as cytochrome C, leading to caspase activation and cell death (13). PUMA can promote apoptosis in various cell types by p53-dependent and -independent mechanisms. In the colon, PUMA is transcriptionally induced by NF-κB in a p53-independent manner to mediate TNF-α–induced apoptosis in IECs (12, 14).

Vitamin D hormone is a pleiotropic hormone with a broad range of biological activities (15). The majority of the body's vitamin D content is derived from photosynthesis in the skin following UV light irradiation (16). Vitamin D is converted to the active hormone 1,25-dihydroxyvitamin D ($1,25(OH)_2D_3$) via 25-hydroxylation in the liver, followed by 1α-hydroxylation in the kidney; the latter is catalyzed by 25-hydroxyvitmain D 1α-hydroxylase (CYP27B1). CYP27B1 is also expressed in extrarenal tissues, including the intestine, to drive local production of $1,25(OH)_2D_3$. Interestingly, colonic *Cyp27B1* expression is influenced by Toll-like receptor activation and colonic inflammation (17, 18). The biological activity of $1,25(OH)_2D_3$ is mediated by the vitamin D receptor (VDR), a member of the nuclear hormone receptor superfamily (19). A growing body of epidemiological data has documented an association between vitamin D deficiency and increased risk of IBD (20–22), including both CD and UC (23–30). A high prevalence of vitamin D deficiency was reported in patients with established as well as newly diagnosed IBD (31–33). Vitamin D deficiency was independently associated with lower quality of life and greater disease activity in IBD (34). Analyses of the large Nurses'

Authorship note: Weicheng Liu and Yunzi Chen contributed equally to this work.
Conflict of interest: The authors have declared that no conflict of interest exists.
Citation for this article: *J Clin Invest.* 2013;123(9):3983–3996. doi:10.1172/JCI65842.

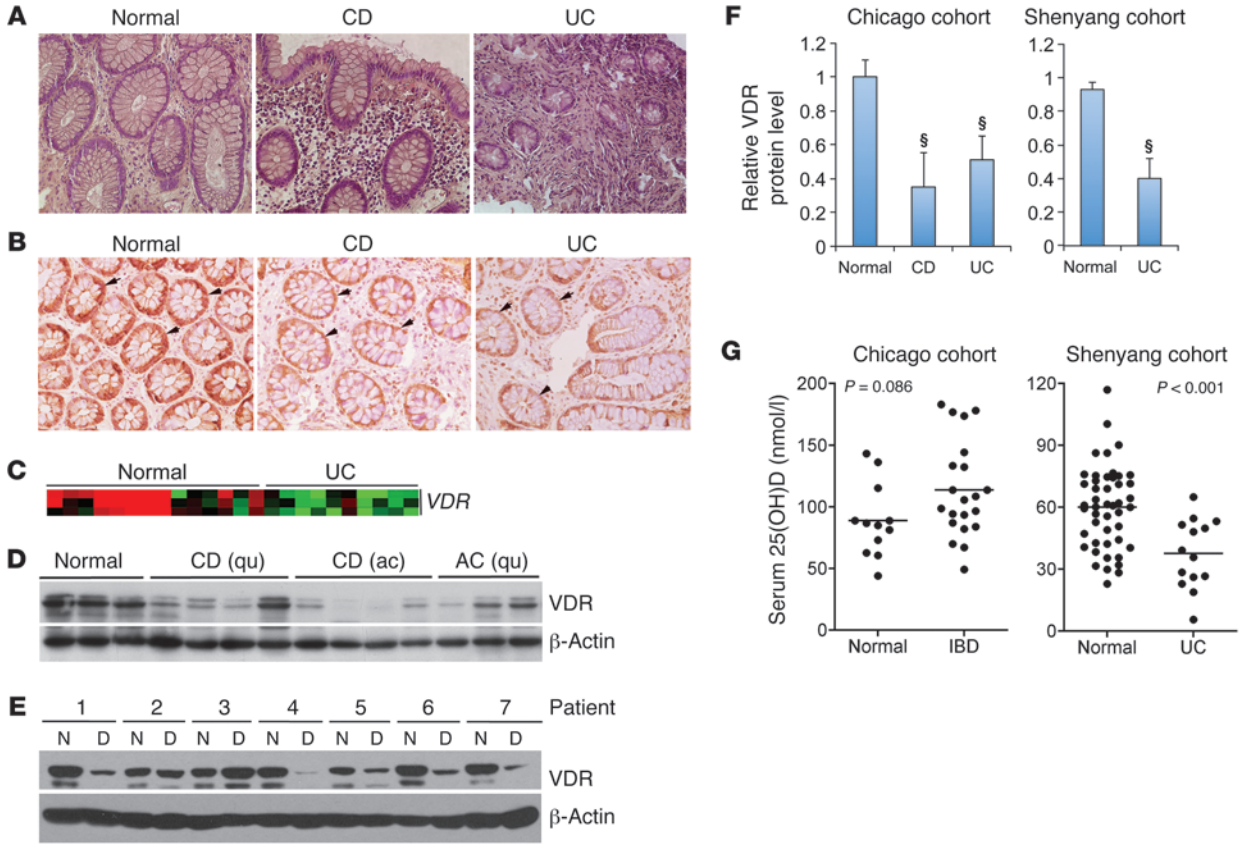

Figure 1

Reduced VDR expression in patients with IBD. (**A**) Representative H&E histology of colonic biopsies obtained from normal subjects and CD and UC patients. Original magnification, ×100. (**B**) Representative immunostaining of colonic biopsies from normal control and CD and UC patients with anti-VDR antibodies. Arrows indicate VDR staining in the epithelial cells. Original magnification, ×100. (**C**) Microarray heatmap showing relative *VDR* transcript levels in normal and UC colonic biopsies. Red color indicates high transcript levels, and green color represents low levels. $n \geq 10$ in each group. (**D**–**F**) Representative Western blots of colonic biopsies from the Chicago cohort (**D**) and the Shenyang cohort (**E**) with anti-VDR antibodies and respective densitometric quantitation (**F**) of VDR protein levels in each cohort (Full, uncut gels are shown in the supplemental material. Supplemental material available online with this article; doi:10.1172/JCI65842DS1). $^{\S}P < 0.001$ versus normal (n = 5–12). Patients are numbered in the Shenyang cohort. ac, active; qu, quiescent; D, diseased lesion tissues; N, normal tissue. (**G**) Serum 25-hydroxyvitamin D concentrations in normal controls and IBD patients from the Chicago and Shenyang cohorts as indicated. Average values are marked by horizontal lines.

Health Study database showed that high vitamin D intake lowered the risk of IBD (35). Moreover, *VDR* gene polymorphisms were reported to be associated with IBD (36–39). These observations suggest that vitamin D status might be an environmental determinant for IBD, whereas VDR status might be a key genetic factor influencing IBD development.

Animal studies have provided evidence for an inhibitory role of vitamin D in the development of IBD. Vitamin D deficiency exacerbated enterocolitis and increased mortality in *Il10*$^{-/-}$ mice, a model of spontaneous colitis, whereas dietary vitamin D supplementation ameliorated colitis and decreased mortality in this model (40). *Vdr*$^{-/-}$/*Il10*$^{-/-}$ mice developed more severe colitis and had higher mortality than *Vdr*$^{+/+}$/*Il10*$^{-/-}$ mice (41). These observations suggest that VDR signaling in the immune cells plays a protective role against IBD. We reported that global VDR deletion increased mucosal injury that led to high mortality in an experimental colitis model (42). In *Vdr*$^{-/-}$ mice, colonic transepithelial electrical resistance, an indicator of epithelial barrier integrity, was significantly reduced before clinical colitis symptoms and histological abnormalities were detected, suggesting that epithelial VDR signaling suppresses colonic inflammation by protecting the integrity of the mucosal barrier. The relative anticolitic contribution of intestinal epithelial VDR signaling and epithelium-independent immune VDR signaling, however, could not be separated in these studies. Here, we used a transgenic approach to specifically address the role of gut epithelial VDR in the pathogenesis of colitis. Our results indicate that epithelial VDR signaling inhibits colitis in part by reducing IEC apoptosis in a manner independent of VDR actions in the non-epithelial immune compartment.

Results

Colonic epithelial VDR levels are markedly reduced in CD and UC patients. Given the potential importance of colonic VDR in IBD pathogenesis, we examined VDR status in colonic biopsies from both CD and UC patients compared with normal colon samples (Figure 1A). Immunostaining with anti-VDR antibodies showed that VDR was highly expressed in normal colonic epithelial cells, but in both CD

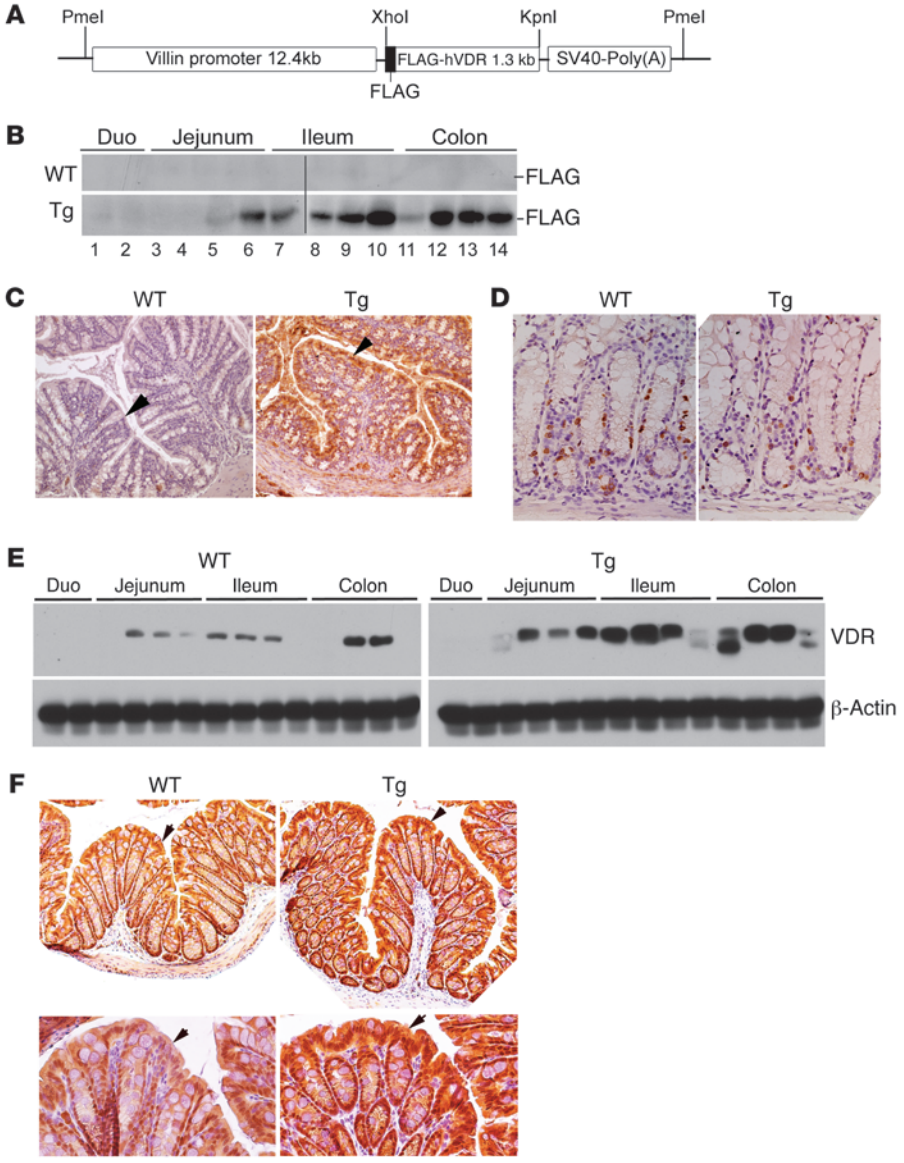

Figure 2
Characterization of *hVDR* Tg mice. (**A**) DNA construct used for pronuclear microinjection to generate *hVDR* Tg mice. (**B**) Western blot using anti-FLAG (–FLAG) antibodies to detect FLAG-hVDR in small and large intestines in WT and Tg mice. Each lane represents 2–3 cm of intestine in the regions indicated. Samples were run together in two gels, which are separated by a black line. Duo, duodenum. (**C**) Immunostaining of large intestine from WT and Tg mice with anti-FLAG antibodies. Arrows indicate the epithelium. Note that only the Tg colon is positively stained. Original magnification, ×100. (**D**) BrdU staining of large intestine from WT and Tg mice. Original magnification, ×200. (**E**) Western blot analysis of WT and Tg small and large intestines using anti-VDR and anti–β-actin antibodies. Each lane represents 2–3 cm of intestine in the regions indicated. (**F**) Immunostaining of large intestine from WT and Tg mice with anti-VDR antibodies. Arrows indicate the crypt epithelium. Original magnification, ×100 (upper panels) and ×200 (lower panels). Note that VDR is predominantly stained in the nuclei.

and UC biopsies, epithelial VDR levels were markedly reduced (Figure 1B). Data from cDNA microarrays (43) confirmed that *VDR* transcript expression was downregulated in UC biopsies ($n \geq 10$) relative to normal colon samples (Figure 1C). To further quantify VDR protein levels and serum vitamin D status in IBD patients, we recruited two cohorts of study subjects, one from Chicago (Illinois, USA), and the other from Shenyang (Liaoning,China). In the Chicago cohort, we found by Western blot analyses that colonic VDR protein levels were significantly reduced in both CD and UC patients compared with normal control subjects (Figure 1, D and F). In active CD biopsies, VDR was lower compared with the quiescent CD biopsies (Figure 1D), suggesting that inflammation may downregulate epithelial VDR expression. In the Shenyang cohort, we collected biopsies from the lesion as well as from the adjacent normal colon tissue in each UC patient (there were very few CD patients available there). In most patients, VDR protein levels were dramatically decreased (by >60% on average) in the lesion relative to the adjacent normal region within the same patient (Figure 1, E and F), whereas proinflammatory cytokine transcripts (*TNFA* and *IL1B*) were elevated in the lesion (not shown). This observation again suggests a repressive effect of local colonic inflammation on epithelial VDR expression.

In the Chicago cohort, the average serum 25-hydroxyvitamin D level in the IBD patients was above the normal range (>75 nmol/l) (Figure 1G), probably reflecting the fact that most of these patients received oral vitamin D supplementation. (When the patients were divided into CD and UC, the mean serum 25-hydroxyvitamin D levels remained normal in each group). In the Shenyang cohort, however, the average serum 25-hydroxyvitamin D level in the UC patients was significantly lower compared with the normal subjects and fell within a severe deficiency range (<50 nmol/l) (Figure 1G). None of the patients in this cohort took vitamin D supplements. These observations suggest that in these patients, the VDR status in the lesion is independent of the serum vitamin D status but is likely affected by the local inflammatory status. The reduction in epithelial VDR could be a causative factor promoting

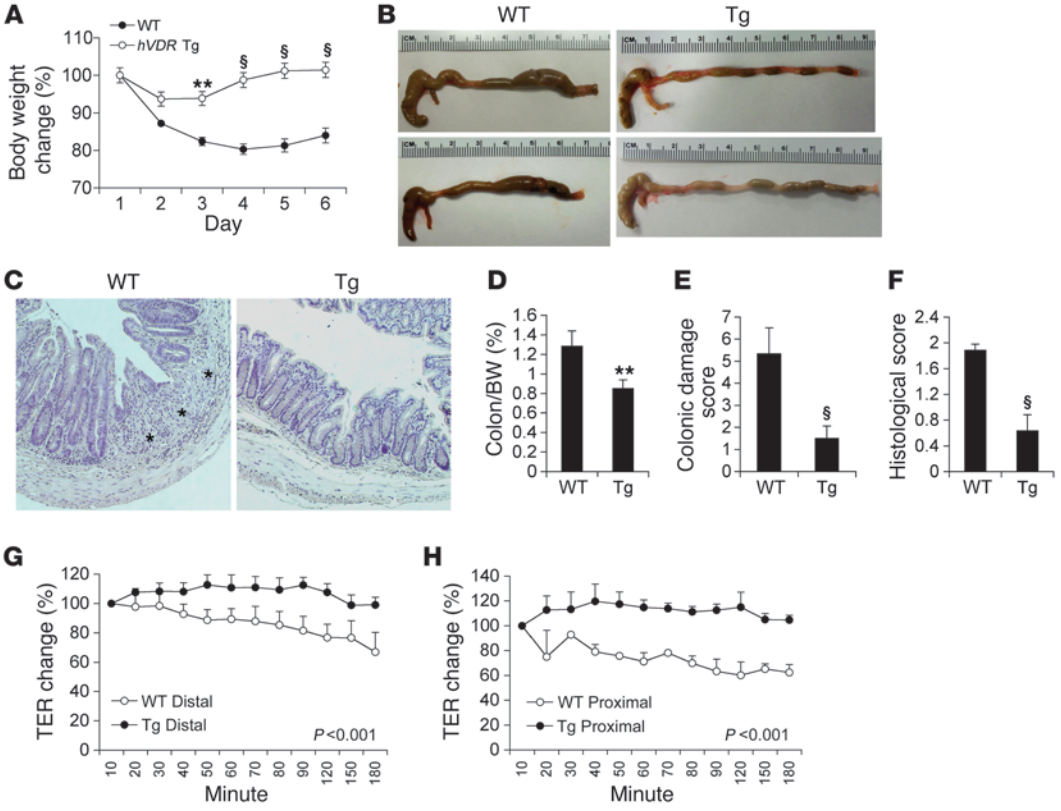

Figure 3
Epithelial hVDR expression protects against TNBS-induced colitis. (**A**) Changes in body weight (percentage of original body weight) over time (days) in WT and Tg mice following TNBS treatment. $^{**}P < 0.01$; $^{§}P < 0.001$ versus WT (n = 7–10). (**B**) Gross morphology of the large intestine from WT and Tg mice on day 6 after TNBS treatment. (**C**) H&E staining of colons from WT and Tg mice on day 6 after TNBS treatment. Note the mucosal ulceration in WT colon, indicated by asterisks. Original magnification, ×100. (**D**–**F**) Colon weight/body weight ratio (**D**), colonic damage score (**E**), and histological score (**F**) of WT and Tg mice on day 6 after TNBS treatment. $^{**}P < 0.01$; $^{§}P < 0.001$ versus WT. n = 5–7 in each genotype. (**G** and **H**) Time course measurement of TER determined by an Ussing chamber study in the distal (**G**) or proximal (**H**) colon from WT and Tg mice on day 2 after TNBS treatment. $P < 0.001$ by log-rank test.

colitis. Therefore, we used a genetic approach to specifically assess the role of epithelial VDR signaling in experimental colitis models.

Generation of transgenic mice that overexpress VDR in intestinal epithelium. To produce Tg mouse lines that express human VDR (hVDR) specifically in IECs, we used the 12.4-kb villin promoter to drive a FLAG-tagged *hVDR* transgene (Figure 2A). The villin promoter has been used to target various transgenes to the intestinal epithelium (44). The FLAG tag, added to the N terminus of hVDR, has no effects on the transactivating activity of hVDR (45), but can distinguish the human transgene from the endogenous mouse VDR. Pronuclear injection of the 14.5-kb PmeI construct (Figure 2A) resulted in four Tg-positive founders on a C57BL/6 background. Three founder lines were mated with WT C57BL/6 mice to obtain germline transmission. Tg lines 3 and 14 were used in this study with comparable results. There was no obvious morphological or growth difference between the WT and Tg mice.

Western blot analyses with anti-FLAG antibodies revealed high expression of FLAG-hVDR from the jejunum to the distal colon in Tg mice (Figure 2B). The transgene expression in the duodenum was very low as reported (44). As expected WT littermates were negative for the FLAG-tagged hVDR (Figure 2B). Immunostaining with anti-FLAG antibodies confirmed that hVDR was predominantly expressed in the intestinal epithelial cells in Tg mice, with the highest level observed in the luminal side of the crypt (Figure 2C). No differences were detected in crypt morphology or cellular proliferation rates between WT and Tg colons, as revealed by BrdU labeling (Figure 2D). Western blotting with anti-VDR antibodies revealed about a 2- to 3-fold increase in VDR levels throughout the intestine in Tg mice relative to the endogenous mouse VDR expression in WT mice (Figure 2E), and immunostaining with anti-VDR antibodies confirmed that this increase was predominately located in the epithelial cells (Figure 2F).

Epithelial hVDR expression protects mice from developing colitis in a TNBS-induced colitis model. To understand the role of epithelial VDR signaling in colitis development, we compared WT and Tg mice using different experimental models of colitis. First, we used the 2,4,6-trinitrobenzene sulfonic acid–induced (TNBS-induced) colitis model, which is believed to resemble CD because it involves T_H1-mediated mucosal inflammation (46). We subjected WT and Tg littermates to TNBS treatment as described (47). Intrarectal instillation of TNBS resulted in gradual weight loss in WT mice during the following 6 days, whereas the weight loss was ameliorated in Tg mice in the first 2 days and quickly recovered in the following days (Figure 3A). By day 6, WT mice

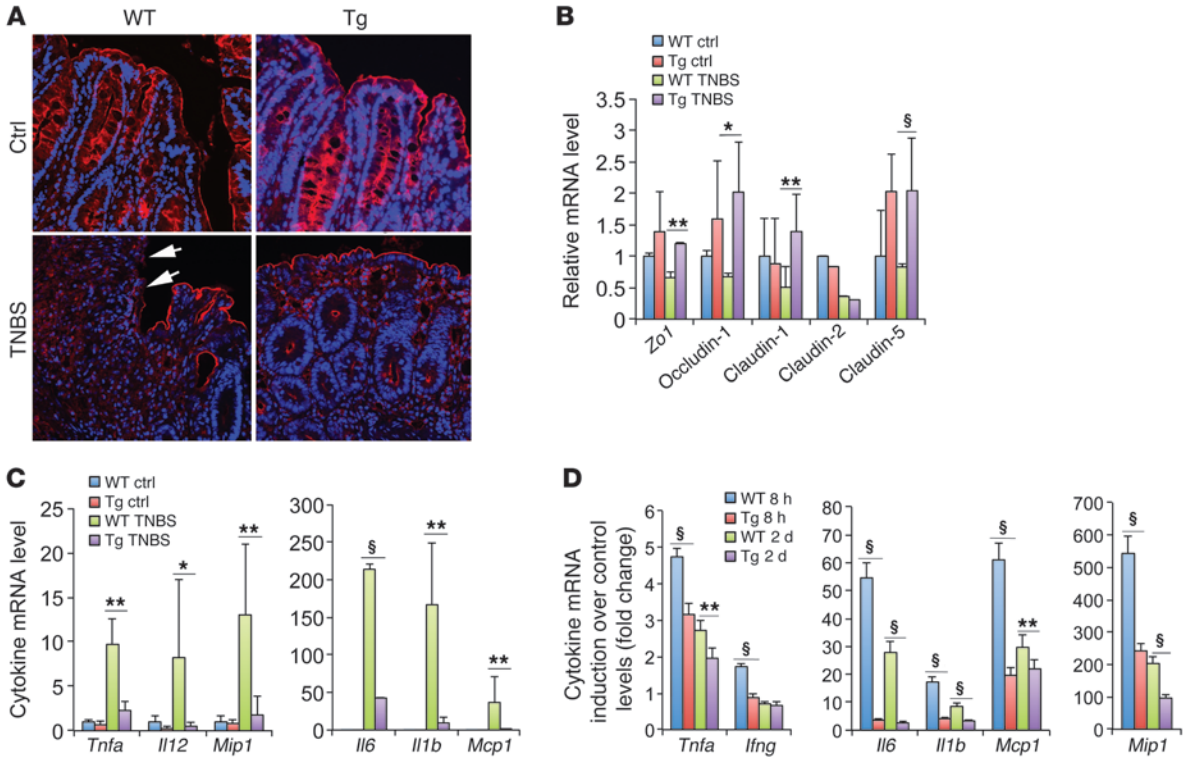

Figure 4

Epithelial hVDR preserves epithelial tight junctions and suppresses colonic inflammation in a TNBS-induced colitis model. (**A**) ZO-1 immunostaining (red) in untreated (Ctrl) and TNBS-treated WT and Tg colons on day 3. Arrows indicate the loss of ZO-1 protein in the luminal epithelium in TNBS-treated WT mice. (**B**) Real-time RT-PCR quantitation of tight junction protein transcripts in control and TNBS-treated WT and Tg colons. (**C**) Real-time RT-PCR quantitation of proinflammatory cytokines and chemokines in colonic mucosa from control and TNBS-treated WT and Tg mice on day 6. (**D**) Fold change induction of proinflammatory cytokines and chemokines in purified colonic epithelial cells from TNBS-treated WT and Tg mice at 8 hours and on day 2 compared with purified untreated control epithelial cells. *$P < 0.05$; **$P < 0.01$; §$P < 0001$. $n = 5$–6 in each genotype.

were symptomatic with severe colitis disease activity, manifested by severe diarrhea and rectal bleeding, and the colon appeared markedly shortened and thickened (Figure 3B). In contrast, Tg mice developed almost no symptoms, and their large bowel showed few signs of colitis (Figure 3B). We performed histological examinations, which confirmed crypt hyperplasia, loss of crypts, severe focal ulceration, and inflammation in the WT colon, along with thickened colonic walls, whereas the Tg colons showed few abnormalities (Figure 3C). Compared with WT mice, Tg mice had significantly lower colon/body weight ratios (Figure 3D), lower colonic damage scores (Figure 3E), and lower histological inflammation scores (Figure 3F) on day 6.

To gain insights into the change in mucosal permeability after TNBS injury, we used an Ussing chamber to measure transepithelial electrical resistance (TER) in the colons obtained from WT and Tg mice 2 days after TNBS treatment. At this time point, we observed no clinical symptoms or histological damage in either genotype. While the TER was markedly reduced in both the distal (Figure 3G) and proximal (Figure 3H) colon from WT mice, the colon mucosal TER was preserved in Tg mice (Figure 3, G and H). These results indicate that epithelial hVDR signaling protects the integrity of the mucosal epithelial barrier.

Next, we examined the colonic epithelial tight junction, which directly affects mucosal permeability. Immunostaining revealed diminished ZO-1 in focal regions in the WT colon 3 days after TNBS treatment, whereas the Tg colon maintained a relatively normal ZO-1 pattern in the epithelium (Figure 4A). Real-time RT-PCR quantitation showed substantial reductions in tight junction protein transcripts (*Zo1*, occludin-1, claudin-1, claudin-2, and claudin-5) in the colonic mucosa of WT mice after TNBS treatment, whereas most of these transcripts were maintained at relatively normal levels in Tg mice (Figure 4B). Moreover, TNBS treatment dramatically induced mucosal proinflammatory cytokines and chemokines (*Tnfa*, *Il1b*, *Il6*, *Il12*, *Mcp1*, and *Mip1*) in WT mice, but the induction of these cytokines and chemokines was substantially attenuated in Tg mice (Figure 4C), confirming that the Tg colon was much less inflamed than the WT colon.

Colonic epithelial cells express Toll-like receptors and can exert an inflammatory response. Since the *hVDR* transgene is only expressed in IECs, we examined the expression of proinflammatory cytokines in colonic epithelial cells immediately purified from WT and Tg mice treated with TNBS for 8 hours and for 2 days, respectively. Relative to untreated control IECs, there was a dramatic induction of *Tnfa*, *Ifng*, *Il6*, *Il1b*, *Mcp1*, and *Mip1* in the WT IECs after 8-hour TNBS treatment, and this induction subsided after 2 days (Figure 4D). In the IECs purified from Tg mice, however, the induction of these cytokines and chemokines was markedly and significantly attenuated at both 8 hours and at 2 days

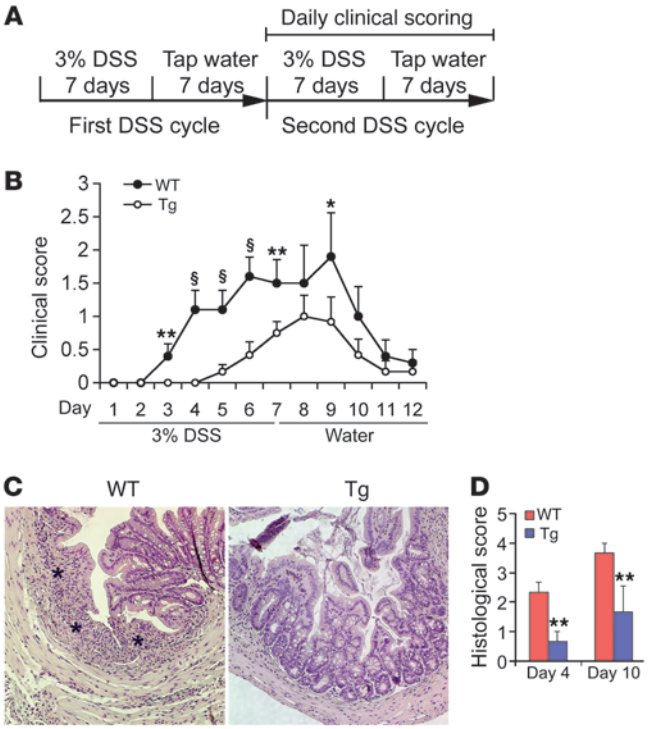

Figure 5
Epithelial hVDR attenuates DSS-induced colitis. (**A**) Schematic illustration of DSS treatment protocol. (**B**) Time course of disease activity index in WT and Tg mice during the second DSS cycle. (**C**) H&E-stained colonic sections from WT and Tg mice on day 10 in the second DSS cycle. Note the severe colonic mucosal ulceration in the WT mice indicated by asterisks. Original magnification, ×100. (**D**) Histologic scores of WT and Tg colons on days 4 and 10 in the second DSS cycle. $^{*}P < 0.05$; $^{**}P < 0.01$; $^{§}P < 0.001$ versus corresponding WT. $n = 6–7$ in each genotype.

(Figure 4D), indicating that hVDR expression within IECs has a direct inhibitory effect on the inflammatory status of the IECs during colitis development.

Epithelial hVDR attenuates colitis in a DSS-induced colitis model. The dextran sulfate sodium–induced (DSS-induced) colitis model resembles human UC with respect to loss of barrier function (48). We then subjected WT and Tg mice to DSS treatment to further assess the anticolitic activity of epithelial VDR signaling. WT and Tg mice received two cycles of DSS treatment provided in drinking water, each cycle consisting of 7 days of water containing DSS followed by 7 days of tap water alone. In the second DSS cycle, the clinical scores were assessed daily (ref. 49 and Figure 5A). WT mice developed clinical symptoms of colitis with increasing severity starting on day 3 in the second cycle and peaking on day 9, whereas symptoms in Tg mice were delayed and significantly reduced in severity (Figure 5B). Histological examination confirmed a marked decrease in immune cell infiltration and ulceration in the Tg colon (Figure 5C), with significantly lower histological scores on days 4 and 10 in the second DSS cycle (Figure 5D). Colonic transcript levels of proinflammatory cytokines were also lower in Tg mice compared with WT mice (not shown). Together, the data from these two chemically induced colitis models indicate that epithelial hVDR expression reduces mucosal barrier damage and prevents colonic inflammation and colitis.

Epithelial hVDR expression blocks colitis in a T cell transfer model of chronic colitis. Chronic gut inflammation is largely mediated by T lymphocytes once initiated by commensal enteric bacterial components. Therefore, the adoptive T cell transfer model of chronic colitis is thought to best recapitulate the clinical and histological characteristics of human IBD (50, 51). We thus selected this model to further examine the effect of epithelial hVDR overexpression on the development of colitis. By breeding *Rag1*$^{-/-}$ (RagKO) and *hVDR* Tg mice, we generated RagKO mice that expressed the FLAG-*hVDR* transgene specifically in the IECs, designated as RagKO Tg mice (Figure 6A). We then compared the development of colitis between RagKO and RagKO Tg mice after injection of $CD4^{+}CD45RB^{hi}$ T cells purified from WT donor mice (50). Approximately 60% of the RagKO mice died of severe colitis by 7 weeks after T cell transfer, whereas only 10% of the RagKO Tg mice died during this period (Figure 6B). Histological examination revealed severe histological damage and colonic inflammation manifested by a large increase in bowel wall thickness, massive leukocyte infiltration, and crypt abscess in the RagKO mice (Figure 6, C and D). In the RagKO Tg mice, we found that colonic inflammation was markedly ameliorated, with a significant reduction in the histological score (Figure 6C). Although crypt hyperplasia was present, we barely detected immune cell infiltration in most of these mice (Figure 6D). We consistently found that colonic proinflammatory cytokine production was substantially attenuated in RagKO Tg mice (Figure 6E). These observations provide very compelling evidence demonstrating that T cell–mediated colonic inflammation can be substantially suppressed by enhancing VDR signaling in the epithelial compartment alone, suggesting that hVDR overexpression strengthens the epithelial barrier function.

Reconstitution of VDR-null epithelial cells with hVDR rescues VDR-null mice from colitis and death. To further assess the anticolitic activity of epithelial VDR signaling, we asked whether reconstituting the IECs of *Vdr*-null mice with the *hVDR* transgene would prevent *Vdr*-null mice from developing colitis. To this end, we generated, through breeding, *Vdr*$^{-/-}$ (VDRKO) mice that expressed hVDR only in the IECs (designated as KO Tg mice). Western blot analyses confirmed the expression of FLAG-hVDR in the colonic mucosa of KO Tg mice, but not of VDRKO mice (Figure 7A). We then examined WT, Tg, VDRKO, and KO Tg mice in parallel using the TNBS and DSS colitis models. In the TNBS model, VDRKO mice developed dramatic weight loss, and all died by day 5 after TNBS treatment (Figure 7, B and C). We found that the colon of VDRKO mice was markedly shortened and swollen (Figure 7D). Histological examination revealed severe ulcerations with complete crypt depletion in the distal colon (Figure 7E, also see Supplemental Figure 1 for whole colon "Swiss roll" images; supplemental material, including full, uncut gels, available online with this article; doi:10.1172/JCI65842DS1). As expected, the colitis phenotype of VDRKO mice was more severe compared with that of WT mice (Figure 7E and Supplemental Figure 1). In contrast, KO Tg mice only developed mild colitis with little weight loss and no death during this period of time (Figure 7, B and C), and their colon showed largely normal gross and histological morphologies (Figure 7, D and E, and Supplemental Figure 1). We consistently found among these four genotypes that VDRKO mice had the highest colonic damage score (Figure 7F) and histological score (Figure 7G), and the highest myeloperoxidase (MPO) activity (Figure 7H) and proin-

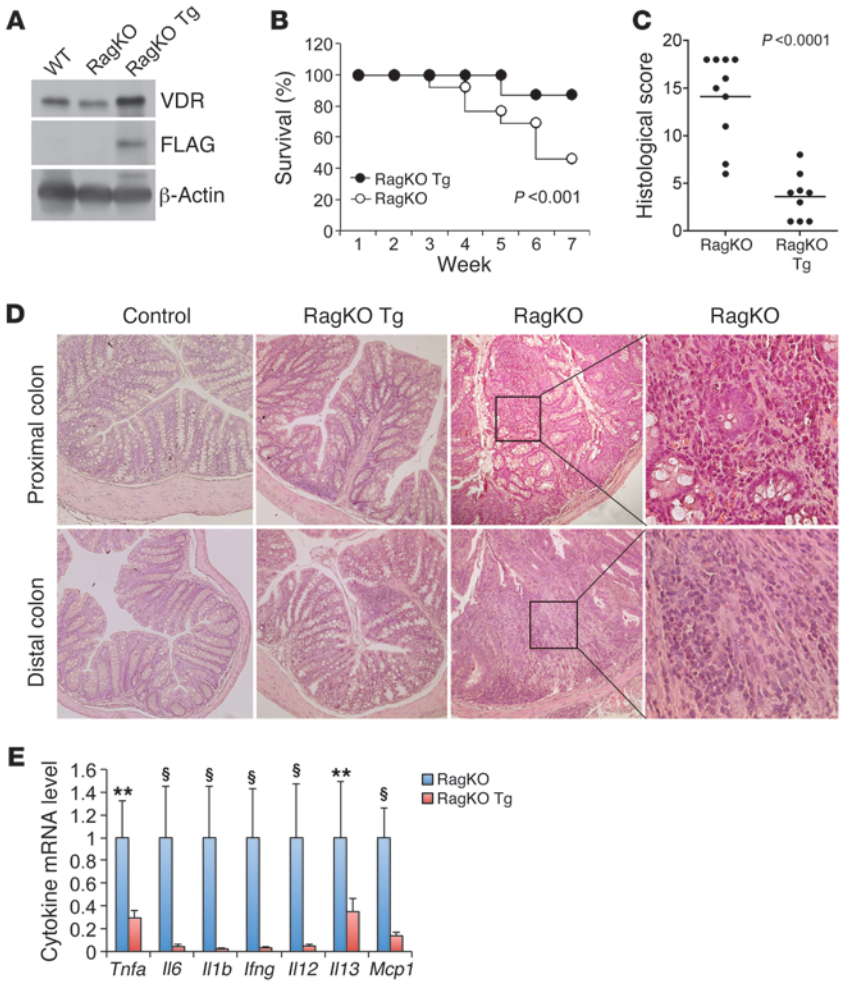

Figure 6
Epithelial hVDR inhibits colitis in a T cell transfer model of chronic colitis. (**A**) Western blot analysis of the colonic mucosa from WT, RagKO, and RagKO Tg mice with anti-VDR and anti-FLAG antibodies. (**B**) Survival curves of RagKO and RagKO Tg mice constituted with $CD4^+CD45RB^{hi}$ T cells. n = 10–12 in each genotype; $P < 0.001$ by log-rank test. (**C**) Colonic histological score in T cell–transferred RagKO and RagKO Tg mice. n = 9–10 in each genotype. Average values are marked by horizontal lines. $P < 0.001$ by a Student's t test. (**D**) H&E-stained proximal and distal colonic sections from T cell–transferred RagKO and RagKO Tg mice. Note the massive leukocyte infiltration in the RagKO colon. Original magnification, ×100. Boxed regions in the RagKO sections are shown at ×400 magnification. (**E**) Relative transcript levels of proinflammatory cytokines and chemokines in the colons of T cell–transferred RagKO and RagKO Tg mice. $^{**}P < 0.01$; $^{§}P < 0.001$ versus corresponding RagKO Tg. n = 5 in each genotype.

flammatory cytokine expression in the colonic mucosa (Figure 7I), but these severe colonic injury and inflammation parameters were almost completely "corrected" in the KO Tg mice (Figure 7, F–I). Similar results were obtained in the DSS colitis model, in which the epithelial *hVDR* transgene was able to substantially reduce animal mortality and clinical scores (Supplemental Figure 2, A and B) and markedly attenuated colonic injury in KO Tg mice compared with VDRKO mice (Supplemental Figure 2C). Taken together, these observations demonstrate that reconstituting only the gut epithelial cells with hVDR is sufficient to rescue *Vdr*-null mice from developing severe colitis despite the presence of a VDR-deficient immune system, confirming a critical and predominant anticolitic role of epithelial VDR signaling in the prevention of colitis.

Epithelial VDR signaling inhibits IEC apoptosis by suppressing PUMA. Increased apoptosis in gut epithelial cells compromises the mucosal barrier, leading to colonic inflammation. By TUNEL staining of WT mice, we observed abundant apoptotic colonic epithelial cells that were further increased in VDRKO mice after TNBS insult, whereas apoptotic epithelial cells were markedly reduced in Tg and KO Tg mice (Figure 8, A and B). In agreement with these observations, we found that caspase 3 cleavage was increased in colonic mucosal lysates from WT and VDRKO mice compared with Tg and KO Tg mice following TNBS treatment (Figure 8, C and D). PUMA, a key mediator of IEC apoptosis, was upregulated in WT mice and even more so in VDRKO mice compared with Tg and KO Tg mice (Figure 8, C and D). In contrast, protein levels of p53, another important regulator of apoptosis, were not altered in these mice (Figure 8, C and D). In the DSS model, PUMA induction (Supplemental Figure 3A) and caspase 3 activation (Supplemental Figure 3B) were also attenuated in the Tg mice. Supporting the relevance of this apoptotic pathway in colitis, we also found that PUMA was upregulated in human CD biopsies (Supplemental Figure 3C). These observations suggest that at least part of the anticolitic mechanism of epithelial VDR signaling involves blocking colonic epithelial cell apoptosis by suppressing PUMA in a p53-independent manner.

Epithelial VDR signaling downregulates PUMA by blocking NF-κB activation in colonic epithelial cells. We used a cell culture system to explore the VDR-dependent mechanism involved in PUMA downregulation. In HCT116 cells, a human colonic cancer cell line, TNF-α markedly induced PUMA, and the induction was attenuated by $1,25(OH)_2D_3$ (Figure 9A). PUMA is regulated by NF-κB, and a functional *cis*-κB site has been identified in the *PUMA* gene promoter (12, 14) (Figure 9B). ChIP assays showed that $1,25(OH)_2D_3$ blocked TNF-α–induced p65 binding to this κB site in HCT116 cells (Figure 9C), and EMSA confirmed that $1,25(OH)_2D_3$ attenuated TNF-α–induced NF-κB binding to the *PUMA* κB probe in HCT116 nuclear extracts (Figure 9D). We have

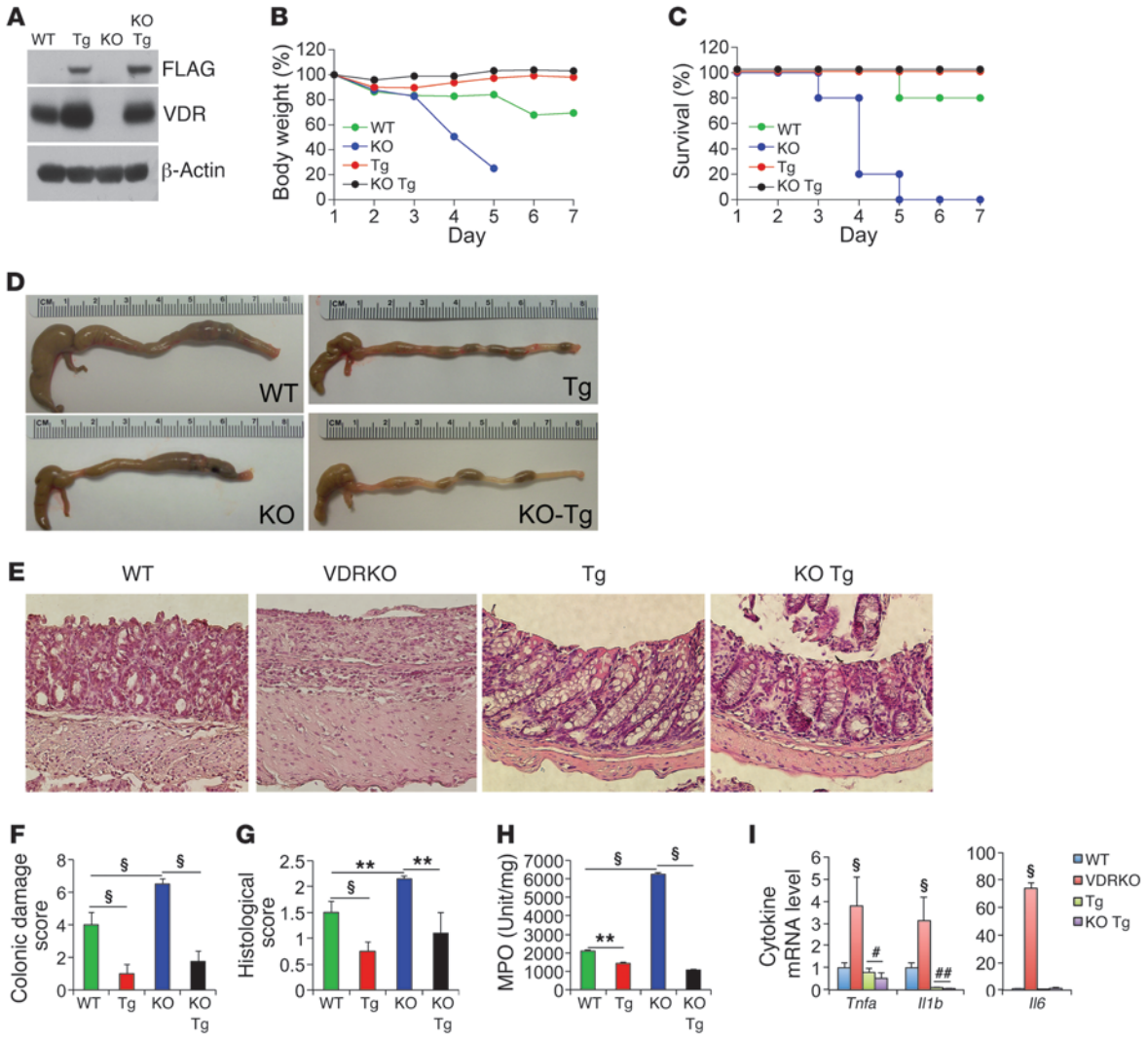

Figure 7

Reconstitution of VDR-null intestinal epithelial cells with the *hVDR* transgene rescues *Vdr*-null mice from colitis and death. WT, VDRKO, Tg, and KO Tg mice were studied in parallel using the TNBS colitis model. (**A**) Western blot analysis of the colonic mucosa from these four genotypes as indicated using anti-FLAG or anti-VDR antibodies. (**B**) Body weight changes over time. (**C**) Survival curves over time. (**D**) Gross morphology of the large intestines on day 6 after TNBS treatment. (**E**) H&E histology of the colons on day 6 after TNBS treatment. Note the severe ulceration in the VDRKO mice, which is inhibited in the KO Tg mice. Original magnification, ×100. (**F**) Colonic damage score; (**G**) histological score; (**H**) MPO activity. $^{**}P < 0.01$; $^{§}P < 0.001$. $n = 7–8$ in each genotype. (**I**) Relative proinflammatory cytokine levels in colonic mucosa of these four genotypes on day 6, quantified by quantitative RT-PCR. $^{§}P < 0.001$ versus the rest; $^{\#}P < 0.05$; $^{\#\#}P < 0.01$ versus WT. $n = 4–5$ in each genotype.

shown previously that $1,25(OH)_2D_3$ suppresses TNF-α–induced NF-κB activity in luciferase reporter assays (52). In HCT116 cells transfected with a luciferase reporter that contains the *PUMA* κB site or its mutant (Figure 9B and ref. 14), $1,25(OH)_2D_3$ treatment inhibited TNF-α–induced luciferase activity with the WT PUMA κB luciferase reporter; for the mutant reporter, however, neither TNF-α nor $1,25(OH)_2D_3$ had effects on the luciferase activity (Figure 9E). To validate that the luciferase activity was indeed mediated by the *PUMA* κB element, we cotransfected HCT116 cells with the PUMA κB luciferase reporter or its mutant and an IKKβ-expressing plasmid or its control plasmid. Transfection of IKKβ dramatically induced the luciferase activity of the WT reporter, but not of the mutant reporter, and this induction was also markedly abrogated by $1,25(OH)_2D_3$ (Figure 9F). Moreover, IKK kinase assays demonstrated that $1,25(OH)_2D_3$ blocked TNF-α–induced IKK activity to phosphorylate IκBα in HCT116 cells (Figure 9G), confirming our previous finding that $1,25(OH)_2D_3$/VDR signaling is able to block NF-κB activation (52–54). To verify that $1,25(OH)_2D_3$ downregulates PUMA by targeting NF-κB activation, we transfected HCT116 cells with an HA-IKKβ–expressing plasmid. IKKβ overexpression induced PUMA, but we found that this PUMA induction could be attenuated by treatment of the cells with $1,25(OH)_2D_3$ (Figure 9H). This result is consistent with our recent finding that liganded VDR blocks NF-κB activation by interacting with IKKβ (55).

To assess whether the epithelial VDR signaling indeed inhibits NF-κB activation in vivo, we measured colonic mucosal IKK kinase activity in WT, Tg, VDRKO, and KO Tg mice with or without TNBS

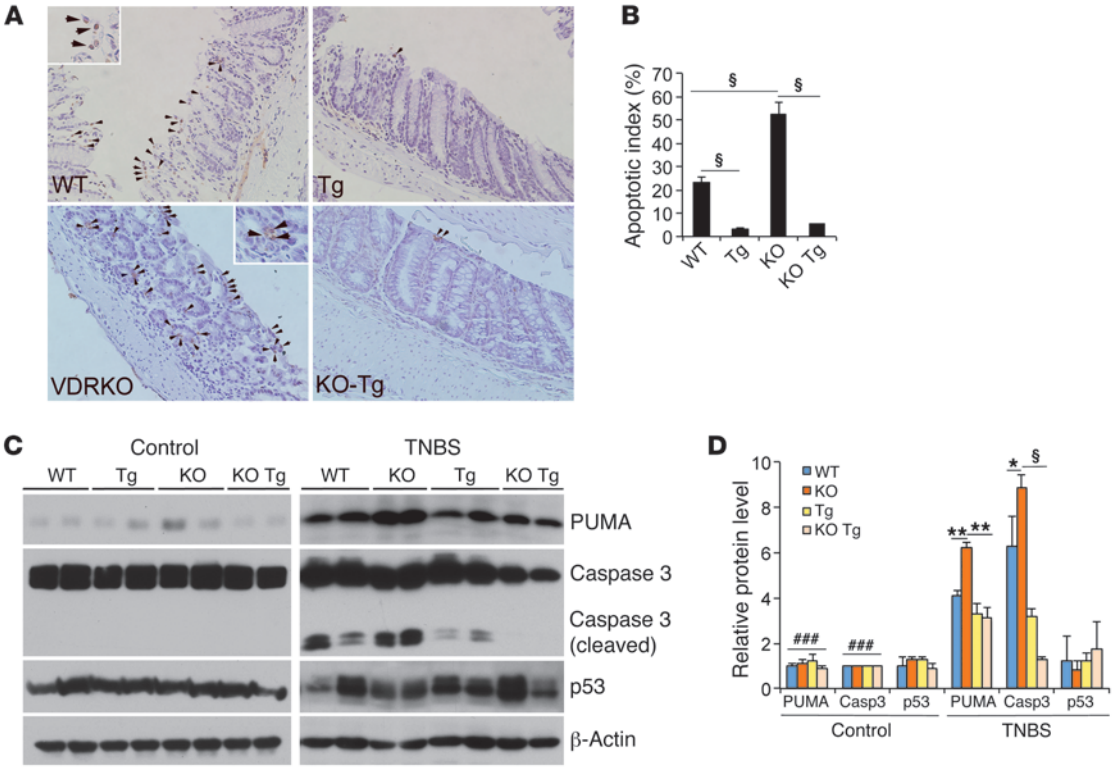

Figure 8

Epithelial VDR signaling attenuates gut epithelial cell apoptosis. WT, VDRKO, Tg, and KO Tg mice were studied in parallel using the TNBS colitis model. (**A**) Representative TUNEL staining of WT, Tg, VDRKO, and KO Tg colons on day 4 after TNBS treatment. Arrows indicate TUNEL-positive apoptotic epithelial cells. Original magnification, ×100 and ×200 (insets). Insets on the WT and VDRKO panels show higher-magnification views of representative TUNEL-positive cells. (**B**) Semiquantitative assessment of epithelial apoptosis. Apoptotic index is the percentage of TUNEL-positive crypts among 80–100 crypts randomly chosen in each genotype. $^{\S}P < 0.001$. (**C** and **D**) Western blot analyses (**C**) and densitometric quantitation (**D**) of colonic mucosal levels of PUMA, caspase 3, and p53 proteins in untreated control and TNBS-treated WT, Tg, VDRKO, and KO Tg mice on day 2. $^{*}P < 0.05$; $^{**}P < 0.01$; $^{\S}P < 0.001$. $^{\#\#\#}P < 0.001$ versus corresponding TNBS-treated colons.

treatment. Two-day TNBS treatment markedly induced colonic mucosal IKK kinase activity in WT mice and even more so in VDRKO mice, and this was accompanied by strong PUMA induction, and caspase 3 activation in WT and VDRKO mice (Figure 9I). Remarkably, the mucosal IKK kinase activity, PUMA induction and caspase 3 activation were all substantially attenuated in Tg and VDRKO Tg mice (Figure 9I). Taken together, these in vitro and in vivo data provide compelling evidence that epithelial VDR signaling inhibits inflammation-induced PUMA expression by blocking NF-κB activation, thereby reducing gut epithelial cell apoptosis.

Discussion

In this study, we found that epithelial VDR levels are substantially reduced in patients with CD and UC and demonstrated in experimental colitis models that gut epithelial VDR signaling has potent anticolitic activity that is independent of nonepithelial immune VDR actions. At least part of the anticolitic mechanism of the epithelial VDR is to inhibit epithelial apoptosis through downregulation of PUMA, a key proapoptotic regulator, and this action results in the protection of the colonic mucosal barrier and hence the reduction of colonic inflammation.

Epidemiological studies have shown that low vitamin D status is common in IBD. Since the major source of vitamin D comes from UV light–driven photosynthesis and dietary components, vitamin D is thought to be an environmental factor that might affect the development of IBD. Studies have suggested that high vitamin D intake is associated with a reduced risk of CD (35), and there are also reports that vitamin D can inhibit colitis in some animal models (40–42); however, whether vitamin D status plays a causative role in the pathogenesis of human IBD is unclear. In this study, we observed very low vitamin D status in one cohort of IBD patients (Shenyang) that did not use vitamin D supplementation and observed relatively normal serum vitamin D levels in another cohort (Chicago) that was routinely supplemented with vitamin D. These results neither include nor exclude low vitamin D status as a causative factor in human IBD. In fact, high serum 1,25-dihydroxyvitamin D status has been reported in a subset of CD patients (56). Future prospective studies are needed to address this issue more conclusively. Despite different serum vitamin D levels, one common feature of these two cohorts is a marked reduction of mucosal epithelial VDR expression. Thus, reduced VDR status in the lesion appears to be an intrinsic characteristic of IBD that is independent of serum vitamin D status. What drives down VDR expression remains to be resolved, but our ongoing preliminary studies suggest that local inflammation is a critical factor in VDR downregulation. In fact, few studies have examined VDR status in the IBD population, but the colonic VDR appears to directly linked to colonic inflammatory status.

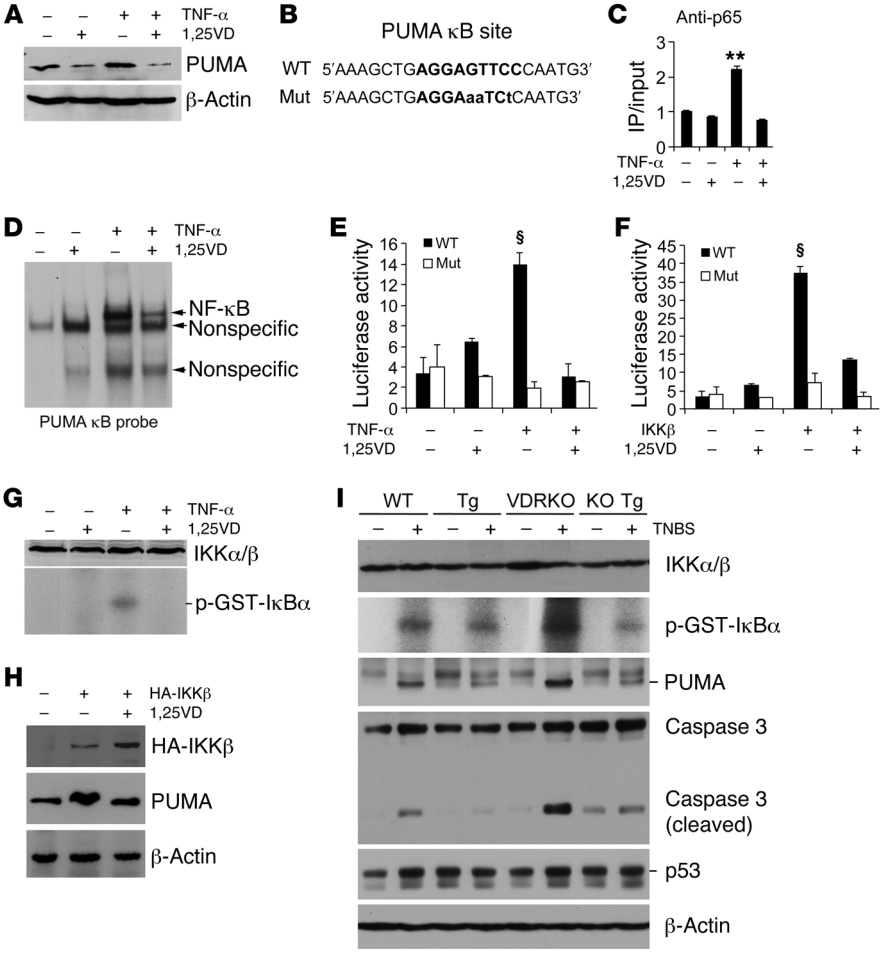

Figure 9

Epithelial VDR signaling abrogates PUMA induction by blocking NF-κB activation. (**A**) Western analysis of PUMA in HCT116 cells treated with TNF-α (100 ng/ml) ± $1,25(OH)_2D_3$ (1,25VD, 20 nM). (**B**) *PUMA* gene promoter κB *cis*-element and its mutant sequences. (**C**) ChIP assay measuring p65 binding to the κB site in HCT116 cells treated with TNF-α ± $1,25(OH)_2D_3$. $^{**}P < 0.01$ versus the rest. (**D**) EMSA using ^{32}P-labeled *PUMA* κB probe and nuclear extracts isolated from HCT116 cells treated with TNF-α ± $1,25(OH)_2D_3$. (**E**) PUMA promoter luciferase reporter assays in HCT116 cells transfected with wild-type (WT) or mutant (Mut) PUMA κB luciferase reporter, followed by treatment with TNF-α ± $1,25(OH)_2D_3$. (**F**) HCT116 cells were cotransfected with the WT or Mut PUMA κB luciferase reporter and IKKβ-expressing plasmid. Luciferase activity was determined after $1,25(OH)_2D_3$ (+) or ethanol (–) treatment. $^{§}P < 0.001$ versus the rest. (**G**) IKK kinase assays in HCT116 cells treated with TNF-α ± $1,25(OH)_2D_3$. (**H**) HCT116 cells were transfected with empty vector (–) or HA-IKKβ plasmid (+), followed by treatment with ethanol (–) or $1,25(OH)_2D_3$ (+). Note that PUMA protein was induced by IKKβ overexpression, and this induction was abolished by $1,25(OH)_2D_3$. (**I**) Colonic mucosal IKK activity. Colonic mucosa were isolated from untreated (–) and TNBS-treated (+) WT, Tg, VDRKO and KO Tg mice on day 2 after TNBS treatment, and the lysates were subjected to IKK kinase assays and Western analyses for IKKα/β, PUMA, caspase 3, and p53 proteins. Each lane represents a pool of 4 to 5 mice of the same genotype and treatment.

VDR is expressed in both the epithelial and nonepithelial compartments of the colon. Given the distinct anatomic and physiological differences between the epithelial and immune compartments in colonic biology, epithelial and nonepithelial VDR signaling may play distinct roles in the pathogenesis of colitis. Our observation of epithelial VDR reduction in diseased colonic regions in both CD and UC patients provides a strong rationale to pursue the role of epithelial VDR signaling in colitis development. In the current study, we employed a genetic approach to address this question. We demonstrated that an approximately 2-fold elevation of VDR expression in gut epithelial cells could render the Tg mice highly resistant to colitis in several different experimental colitis models, including the TNBS and DSS models, in which acute colitis is induced chemically, and the adoptive T cell transfer model, in which chronic colitis is induced by the disruption of T cell homeostasis. TNBS is thought to haptenize colonic autologous or microbiota proteins, rendering them immunogenic to the host immune system, inducing T cell–mediated colonic inflammation (57). Thus, the TNBS model is believed to resemble CD in humans. DSS is toxic to the gut epithelial cells and induces colitis by disruption of the mucosal epithelial barrier. Mice treated with DSS develop colitis resembling UC in humans (48). The adoptive T cell transfer model closely recapitulates the clinical and histopathological features of human CD, including transmural inflammation, epithelial hyperplasia, leukocyte infiltration, crypt abscesses, and epithelial cell erosions (50). Therefore, the clinical relevance of our animal observations is sound. In all these models, Tg mice overexpressing hVDR showed a remarkable reduction in colonic inflammation and colonic injury compared with their WT counterparts, as assessed by clinical, morphological, pathohistological, and molecular parameters. At the early phase, WT mice exhibited increased mucosal permeability prior to detectable morphological and histological abnormalities, but Tg mice maintained relatively normal permeability as well as relatively normal levels of tight junction proteins. Proinflammatory cytokines in the gut epithelial cells were also suppressed. At late stages, the severe colitis phenotype seen in WT mice, such as ulceration and massive leukocyte infiltration, was mostly absent in Tg mice. Together, our data suggest that the potent anticolitic activity of epithelial VDR signaling is derived at least in part from reducing the inflammatory status of the epithelial cells and maintaining the integrity of the mucosal epithelial barrier.

We have previously reported that genetic *Vdr* deletion leads to severe colitis in the DSS model (42). Because the mutant mice carried global deletion of the *Vdr* gene, the relative contribution of epithelial and nonepithelial VDR signaling in the development of colitis was indistinguishable. We reasoned that if the anticolitic activity of the epithelial VDR is a primary and essential protective mechanism, then reconstitution of the *Vdr*-deficient gut

epithelial cells in *Vdr*$^{-/-}$ mice with the *hVDR* transgene should be able to prevent or attenuate the severe colitic phenotype seen in *Vdr*$^{-/-}$ mice, even though the immune system remains *Vdr* deficient. Indeed, we observed that while VDRKO mice developed very severe colitis leading to high mortality following either TNBS or DSS insult, the KO Tg mice were highly resistant to colitis, with marked attenuation of colonic inflammation and no death in both experimental models. Relatively normal crypt architecture was maintained in these mice. Given that the KO Tg mice still have a *Vdr*-deficient immune system that is hyperresponsive to immune stimuli, since immune VDR signaling suppresses inflammatory response (58), we conclude that enhanced epithelial VDR signaling is sufficient to inhibit colitis, regardless of the VDR status in the nonepithelial immune system.

Vitamin D has immune-modulatory activities (59, 60), and the VDR-deficient immune system was thought to be the main promoter for the robust colitis phenotype seen in *Il10/Vdr* double-mutant mice (41). IBD is a chronic inflammatory disorder, and there is little doubt that immune VDR signaling can exert anticolitic effects by downgrading proinflammatory reactions. As such, immune *Vdr* deficiency could render the colonic immune components hyperreactive to invading luminal antigens or bacteria, leading to hypercolonic inflammation. Our study suggests, however, that epithelial VDR signaling functions as a primary defense mechanism to suppress colonic inflammation by maintaining an intact and functional mucosal barrier, which prevents luminal antigens and bacteria from interacting with the immune components in the lamina propria. As such, when the *Vdr*-deficient gut epithelial cells were reconstituted with the *hVDR* transgene, the integrity of the mucosal barrier was restored to prevent the otherwise hyperinflammatory response in the VDR-deficient lamina propria immune cells. We believe these data demonstrate for the first time that the anticolitic activity of the epithelial VDR is independent of VDR actions in the nonepithelial compartment. Therefore, the reduction of epithelial VDR observed in IBD patients is predicted to compromise the epithelial barrier and thus likely contributes to the development of IBD. One limitation of this study is that the gain-of-function approach that we took cannot directly address whether the 50%–60% reduction in epithelial VDR levels we observed in IBD patients would have a major impact on colonic inflammation. It might be more appropriate to use an epithelium-specific loss-of-function approach to address this issue in the future.

How does the epithelial VDR protect the mucosal barrier? In this study, we showed that epithelial VDR signaling inhibits gut epithelial cell apoptosis by downregulating PUMA. It is well understood that increased gut epithelial apoptosis compromises the mucosal barrier and increases mucosal permeability. In our colitis models, extensive colonocyte apoptosis was detected in WT mice and more so in *Vdr*-null mice, accompanied by robust PUMA induction and caspase 3 activation, but epithelial expression of hVDR in either a *Vdr* WT or a null background markedly suppressed PUMA upregulation and caspase 3 activation, leading to a reduction in IEC apoptosis. The increase in colonic epithelial apoptosis appeared to be p53 independent (12).

Since PUMA is a key inducer of gut epithelial apoptosis, we embarked on studies to dissect the molecular mechanism whereby $1,25(OH)_2D_3$-VDR downregulates *PUMA* expression. In IECs, NF-κB mediates inflammation-induced PUMA upregulation (14). Here, we demonstrated that $1,25(OH)_2D_3$ abrogates PUMA induction by blocking NF-κB activation. This conclusion is based on several lines of in vitro and in vivo evidence. In HCT116 cells, $1,25(OH)_2D_3$ inhibited TNF-α–induced PUMA protein and *PUMA* promoter activity, and this inhibition was mediated by the κB *cis*-DNA element in the *PUMA* gene promoter. To directly link vitamin D actions to the blockade of NF-κB activation, we showed that $1,25(OH)_2D_3$ attenuated IKKβ-induced *PUMA* promoter activity and PUMA protein expression, inhibited TNF-α–induced IKK kinase activity, and disrupted TNF-α–induced p65 binding to the *PUMA* κB site. Importantly, we further demonstrated that hVDR expression in gut epithelial cells substantially inhibited IKK kinase activity in colonic mucosa from either Tg or KO Tg mice, together with the inhibition of PUMA induction and caspase 3 activation. These data confirm that VDR signaling suppresses epithelial NF-κB activity in vivo, providing mechanistic insights into the function of epithelial VDR signaling in colonic homeostasis. Our recent studies showed that VDR is able to directly interact with IKKβ protein to attenuate NF-κB activation (55).

Colonic commensal bacteria play a key role in the development of IBD. Colonic epithelial cells influence the microbiota by secreting antimicrobial peptides (61). Vitamin D has been reported to induce cathelicidin and β2-defensins (62, 63). It is conceivable that epithelial VDR can regulate colonic inflammation by regulating antimicrobial peptide production in colonocytes. Moreover, epithelial VDR signaling may also regulate autophagy, another molecular event that has been implicated in IBD (64, 65). Indeed, vitamin D/VDR signaling is known to regulate autophagy (66). In this study, we showed that VDR overexpression also inhibited epithelial inflammatory cytokine production in IBD models, which may have a significant impact on the course of colonic inflammation. The inflammatory cytokines produced by the epithelial cells have autocrine and paracrine effects in the colon. These potential anticolitic mechanisms warrant further investigation in the future. It is conceivable that the anticolitic mechanism of epithelial VDR signaling is multifactorial and not limited to the regulation of barrier function.

In conclusion, in this report we provide strong evidence that epithelial VDR signaling inhibits colitis by protecting the mucosal epithelial barrier, and this anticolitic activity is independent of VDR actions in the nonepithelial immune system. Given the relatively deficient VDR status observed in IBD patients, targeting VDR expression in epithelial cells might be a useful strategy for the treatment of IBD.

Methods

Human biopsies. Patients with IBD and non-IBD control subjects were recruited with written informed consent for this study at the University of Chicago Medical Center and at Shenjing Hospital of China Medical University. The non-IBD controls were patients who underwent screening colonoscopies without active gastrointestinal pathology. The diagnosis of CD or UC was based on a standard combination of clinical, endoscopic, histological, and radiological criteria. The severity of macroscopic inflammation of the colon mucosa at colonoscopy was graded according to the Mayo score for UC (67) and the disease endoscopic index of severity (CDEIS) subscore for CD (68). In the Shenyang cohort, we collected colonic biopsies from the lesion and adjacent normal tissue from each patient. We subjected the biopsies to histological and anti-VDR immunohistochemical analyses. Tissue lysates were also prepared from the biopsies for Western blot analyses. Data for human *VDR* transcript levels in colonic mucosal biopsies of normal control subjects and UC patients

without dysplasia were obtained from previously published microarray data (43) deposited in the NCBI's Gene Expression Omnibus repository (GEO accession number GSE37283).

Transgenic mice. FLAG-hVDR was generated by adding the FLAG nucleotide sequence to the N terminus of the hVDR cDNA coding sequence as described (45). The FLAG-hVDR cDNA (1.3 kb) was placed under the control of the 12.4-kb mouse villin gene promoter (44) (provided by Deborah Gumucio, University of Michigan, Ann Arbor, Michigan, USA), followed by the SV40 T antigen poly(A) sequence. The 14.5-kb PmeI-PmeI DNA construct was purified and used for pronuclear microinjection, which was carried out by the Transgenic Mouse Core Facility at the University of Chicago using a C57BL/6 genetic background. Pups born from the microinjection were screened by PCR-based genotyping using hVDR-specific primers. Transgene-positive mice were crossed with C57BL/6 mice to obtain germ line transmission. *Vdr*$^{-/-}$ mice have been described previously (69). *Vdr*$^{-/-}$ mice that expressed the *hVDR* transgene (KO Tg mice) were obtained from crossing *hVDR* Tg and *Vdr*$^{+/-}$ mice, followed by breeding between *Vdr*$^{+/-}$ Tg and *Vdr*$^{+/-}$ mice. *Rag1*$^{-/-}$ mice that expressed the *hVDR* transgene (RagKO Tg) were obtained from crossing *Rag1*$^{-/-}$ with *hVDR* Tg mice to obtain *Rag1*$^{+/-}$ Tg mice, followed by breeding between *Rag1*$^{-/-}$ and *Rag1*$^{+/-}$ Tg mice. All mice were on a C57BL/6 background.

Chemically induced colitis models. Eight- to 12-week-old mice were studied using TNBS-induced and DSS-induced colitis models as described (47). For the TNBS model, overnight-fasted mice were treated under anesthesia with 100 mg/kg TNBS (Sigma-Aldrich) dissolved in 50% alcohol via intrarectal injection using a 1-ml syringe fitted with an 18-gauge stainless steel gavage needle, with 50% alcohol treatment as a control. For the DSS model, mice were provided 2%–3% DSS (Fisher Scientific) dissolved in the drinking water for 2 cycles, each cycle consisting of 7 days of DSS water and 7 days of tap water. Body weights, stool consistency, and GI bleeding were monitored daily. Clinical scores and colonic damage scores were estimated as detailed previously (49, 70–72). Colons were collected immediately after sacrifice, and mucosa was scraped to isolate total RNA or proteins. Colonic histological analyses were performed using the "Swiss roll" method (73) or using bread-loafing cross sections, and histological scores were graded according to a previously published system (72, 74). Colonic TER was determined in freshly harvested colons using an Ussing chamber as described (42, 74).

Adoptive T cell transfer model of chronic colitis. RagKO and RagKO Tg mice were studied in parallel using the T cell transfer colitis model according to a protocol previously published, with modifications (50). Briefly, spleen cell suspensions were prepared from WT donor mice, and CD4$^+$ T cells were enriched by depleting non-CD4$^+$ cells using a mouse CD4$^+$ T Cell Isolation Kit II (Miltenyi Biotec). This was achieved by magnetically labeling non-CD4$^+$ cells with a cocktail of biotin-conjugated monoclonal antibodies and anti-biotin MicroBeads (Miltenyi Biotec), followed by removing these non-CD4$^+$ cells using the MACS separation system (Miltenyi Biotec). The enriched CD4$^+$ T cells were incubated with anti-mouse CD4-FITC and anti-mouse CD45RB-PE antibodies (eBioscience), and the CD4$^+$CD45RB^{hi} T cells were sorted by FACS. RagKO and RagKO Tg recipient mice were injected i.p. with FACS-purified CD4$^+$CD45RB^{hi} T cells (0.5×10^6 cells per mouse). Mouse colitis phenotypes were analyzed and scored as detailed previously (50).

Isolation of colonic epithelial cells. Colonic epithelial cells were isolated from freshly harvested colons using Percoll gradient centrifugation according to the procedure described previously (75). Briefly, colons were cut into 0.5-cm segments and incubated in HBSS containing 5% FBS, 1 mM DTT, and 0.5 mM EDTA (pH 8.0) at 37°C for 45 minutes in an orbital shaker. The supernatant was filtered through a 100-μm sieve, and epithelial cells were purified by centrifugation through a 25%/40% discontinuous Percoll gradient. The purified cells were immediately used to extract total RNA.

TUNEL staining. TUNEL staining was performed with an ApopTag Plus Peroxidase In Situ Apoptosis Detection Kit (Millipore) according to the manufacturer's instructions. Apoptosis was semiquantified by assessing TUNEL-positive crypts in 80 to 100 randomly chosen crypts in each mouse, and the apoptotic index was defined as the percentage of TUNEL-positive cell-containing crypts, as previously described (12).

Histology and immunohistochemical staining. Freshly dissected colon or colon biopsies were fixed overnight with 4% formaldehyde in PBS (pH 7.2), processed, and embedded in paraffin wax. Tissues were cut into 4-μm sections. Colonic morphology was examined by H&E staining. To localize hVDR and VDR expression, sections were stained with anti-FLAG (Sigma-Aldrich) or anti-VDR (Santa Cruz Biotechnology Inc.) antibodies as primary antibodies, followed by staining with horseradish peroxidase-conjugated anti-IgG as second antibodies. Antigens were then visualized with 3,3′-diaminobenzidine substrate (Sigma-Aldrich) and observed under a light microscope.

Measurement of serum 25-hydroxyvitamin D. Human serum 25-hydroxyvitamin D levels were determined using a commercial 25-hydroxyvitamin D EIA kit (Immunodiagnostic Systems) according to the manufacturer's instructions.

Cell culture and treatment. HCT116 cells were grown in DMEM supplemented with 10% FBS. Cells were usually treated with or without 100 ng/ml TNF-α for 0 to 72 hours in the presence of 20 nM $1,25(OH)_2D_3$ or ethanol (vehicle) as specified in each experiment, followed by isolation of the total RNA or protein lysates for analyses.

RT-PCR. Total RNA was extracted using TRIzol reagents (Invitrogen). First-strand cDNAs were synthesized using a ThermoScript RT kit (Invitrogen). Conventional PCR was carried out in a BioRad DNA Engine. Real-time PCR was performed in a Roche 480 Real-Time PCR system using SYBR green PCR reagent kits (Clontech). The relative amount of transcripts was calculated using the $2^{-\Delta\Delta Ct}$ formula as described previously (76). PCR primers are provided in Supplemental Table 1.

Western blotting. Proteins were separated by SDS-PAGE and electroblotted onto Immobilon-P membranes (Millipore). Western blotting analyses were carried out as previously described (77). The antibodies used in this study included: VDR, IκBα, IKKβ, IKKα/β (all from Santa Cruz Biotechnology Inc.), FLAG, β-actin (Sigma-Aldrich), PUMA (Abcam), caspase 3, and p53 (both from Cell Signaling Technology).

Kinase assays. IκB kinase (IKK) assays were performed as described (78). Briefly, lysates prepared from HCT116 cells or colonic mucosa were immunoprecipitated with anti-IKKγ antibodies (Santa Cruz Biotechnology Inc.). The precipitant was incubated with recombinant GST-IκBα (amino acids 1–54; Clontech) in the presence of γ-^{32}P-ATP, and ^{32}P-labeled GST-IκBα (amino acids 1–54) was detected by autoradiography as described previously (58).

Luciferase reporter assays. HCT116 cells were transfected with PUMA κB luciferase reporter plasmid or its mutant (14) (provided by Lin Zhang, University of Pittsburgh, Pittsburgh, Pennsylvania, USA) or cotransfected with this plasmid and IKKβ-expressing plasmid using Lipofectamine 2000 (Invitrogen). After overnight culture, the transfected cells were treated with or without TNF-α (100 ng/ml) in the presence of $1,25(OH)_2D_3$ (20 nM) or ethanol as indicated in the experiment. Luciferase activity was determined using the Dual-Luciferase Reporter Assay System (Promega) as reported previously (79).

ChIP assays. ChIP assays were performed as described previously (79) using anti-p65 antibodies. The assays were quantified by real-time PCR using primers (Supplemental Table 1) flanking the κB site in the promoter of the *PUMA* gene as described (14).

EMSA. Nuclear extracts were prepared from HCT116 cells treated overnight with or without TNF-α (100 ng/ml) in the presence of $1,25(OH)_2D_3$ (20 nM) or ethanol as described (79). The nuclear extracts were incubated with a ^{32}P-labeled double-stranded *PUMA* κB probe (5′-AAGCTGAGGAGTTCCCAATG-3′), and EMSA was performed as described previously (79).

Statistics. Data values were presented as the means ± SEM. Statistical comparisons were performed using an unpaired 2-tailed Student's *t* test or a 1-way ANOVA, as appropriate, with $P < 0.05$ considered statistically significant.

Study approval. The collection of human colonic biopsies and blood was approved by the IRBs of The University of Chicago (Chicago, Illinois, USA) and by the Institutional Ethical Committee of China Medical University (Shenyang, Liaoning, China), respectively. Study subjects were recruited with written informed consent obtained from the participants or their guardians. All animal studies were approved by the IACUC of The University of Chicago.

Acknowledgments

We thank Lin Zhang (University of Pittsburgh, Pittsburgh, Pennsylvania, USA) for providing the PUMA κB luciferase reporter plasmid and Deborah Gumucio (University of Michigan, Ann Arbor, Michigan, USA) for providing the villin promoter plasmid. This work was supported by NIH grants HL085793 and NIDDK P30DK42086 (DDRCC); by research grants from the Gastrointestinal Research Foundation (GIRF) Associate Board; the Foundation for Clinical Research in Inflammatory Bowel Disease (FCRIBD); and the International Organization for the Study of Inflammatory Bowel Disease (IOIBD); and by a research grant from the Liaoning Government (China). The production of villin-*hVDR* transgenic mice was supported in part by CTSA grant UL1 RR024999 from the National Center for Research Resources (NCRR). The University of Chicago Transgenic Mouse Core Facility was supported in part by NIH grant 5P30CA014599-36. W. Liu was partly supported by the Kohut fund. M.A. Golan was partly supported by a Goldgraber fellowship.

Received for publication May 13, 2013, and accepted in revised form June 21, 2013.

Address correspondence to: Yan Chun Li, Department of Medicine, The University of Chicago, 900 E. 57th Street, KCBD, Mailbox 9110, Chicago, Illinois 60637, USA. Phone: 773.702.2477; Fax: 773.702.2281; E-mail: cyan@medicine.bsd.uchicago.edu.

1. Podolsky DK. Inflammatory bowel disease. *N Engl J Med*. 2002;347(6):417–429.
2. Gibson PR. Increased gut permeability in Crohn's disease: is TNF the link? *Gut*. 2004;53(12):1724–1725.
3. Laukoetter MG, Bruewer M, Nusrat A. Regulation of the intestinal epithelial barrier by the apical junctional complex. *Curr Opin Gastroenterol*. 2006;22(2):85–89.
4. Watson AJ, et al. Epithelial barrier function in vivo is sustained despite gaps in epithelial layers. *Gastroenterology*. 2005;129(3):902–912.
5. Fasano A, Shea-Donohue T. Mechanisms of disease: the role of intestinal barrier function in the pathogenesis of gastrointestinal autoimmune diseases. *Nat Clin Pract Gastroenterol Hepatol*. 2005;2(9):416–422.
6. Di Sabatino A, et al. Increased enterocyte apoptosis in inflamed areas of Crohn's disease. *Dis Colon Rectum*. 2003;46(11):1498–1507.
7. Hagiwara C, Tanaka M, Kudo H. Increase in colorectal epithelial apoptotic cells in patients with ulcerative colitis ultimately requiring surgery. *J Gastroenterol Hepatol*. 2002;17(7):758–764.
8. Iwamoto M, Koji T, Makiyama K, Kobayashi N, Nakane PK. Apoptosis of crypt epithelial cells in ulcerative colitis. *J Pathol*. 1996;180(2):152–159.
9. Frey MR, Edelblum KL, Mullane MT, Liang D, Polk DB. The ErbB4 growth factor receptor is required for colon epithelial cell survival in the presence of TNF. *Gastroenterology*. 2009;136(1):217–226.
10. Nenci A, et al. Epithelial NEMO links innate immunity to chronic intestinal inflammation. *Nature*. 2007;446(7135):557–561.
11. Edelblum KL, Yan F, Yamaoka T, Polk DB. Regulation of apoptosis during homeostasis and disease in the intestinal epithelium. *Inflamm Bowel Dis*. 2006; 12(5):413–424.
12. Qiu W, et al. PUMA-mediated intestinal epithelial apoptosis contributes to ulcerative colitis in humans and mice. *J Clin Invest*. 2011;121(5):1722–1732.
13. Yu J, Zhang L. PUMA, a potent killer with or without p53. *Oncogene*. 2009;27(suppl 1):S71–S83.
14. Wang P, et al. PUMA is directly activated by NF-kappaB and contributes to TNF-alpha-induced apoptosis. *Cell Death Differ*. 2009;16(9):1192–1202.
15. Bouillon R, et al. Vitamin D and human health: lessons from vitamin D receptor null mice. *Endocr Rev*. 2008;29(6):726–776.
16. Holick MF. Vitamin D deficiency. *N Engl J Med*. 2007;357(3):266–281.
17. Liu N, et al. Altered endocrine and autocrine metabolism of vitamin D in a mouse model of gastrointestinal inflammation. *Endocrinology*. 2008; 149(10):4799–4808.
18. Mukherji A, Kobiita A, Ye T, Chambon P. Homeostasis in intestinal epithelium is orchestrated by the circadian clock and microbiota cues transduced by TLRs. *Cell*. 2013;153(4):812–827.
19. Haussler MR, et al. The nuclear vitamin D receptor: biological and molecular regulatory properties revealed. *J Bone Miner Res*. 1998;13(3):325–349.
20. Loftus EV Jr, Sandborn WJ. Epidemiology of inflammatory bowel disease. *Gastroenterol Clin North Am*. 2002;31(1):1–20.
21. Loftus EV Jr. Clinical epidemiology of inflammatory bowel disease: Incidence, prevalence, and environmental influences. *Gastroenterology*. 2004; 126(6):1504–1517.
22. Lim WC, Hanauer SB, Li YC. Mechanisms of disease: vitamin D and inflammatory bowel disease. *Nat Clin Pract Gastroenterol Hepatol*. 2005;2(7):308–315.
23. Bischoff SC, Herrmann A, Goke M, Manns MP, von zur Muhlen A, Brabant G. Altered bone metabolism in inflammatory bowel disease. *Am J Gastroenterol*. 1997;92(7):1157–1163.
24. Jahnsen J, Falch JA, Mowinckel P, Aadland E. Vitamin D status, parathyroid hormone and bone mineral density in patients with inflammatory bowel disease. *Scand J Gastroenterol*. 2002;37(2):192–199.
25. Marx G, Seidman EG. Inflammatory bowel disease in pediatric patients. *Curr Opin Gastroenterol*. 1999;15(4):322–325.
26. Pappa HM, et al. Vitamin D status in children and young adults with inflammatory bowel disease. *Pediatrics*. 2006;118(5):1950–1961.
27. Scharla SH, et al. Bone mineral density and calcium regulating hormones in patients with inflammatory bowel disease (Crohn's disease and ulcerative colitis). *Exp Clin Endocrinol*. 1994;102(1):44–49.
28. Schulte CM. Review article: bone disease in inflammatory bowel disease. *Aliment Pharmacol Ther*. 2004;20(suppl 4):43–49.
29. Sinnott BP, Licata AA. Assessment of bone and mineral metabolism in inflammatory bowel disease: case series and review. *Endocr Pract*. 2006;12(6):622–629.
30. Souza HN, Lora FL, Kulak CA, Manas NC, Amarante HM, Borba VZ. [Low levels of 25-hydroxyvitamin D (25OHD) in patients with inflammatory bowel disease and its correlation with bone mineral density]. *Arq Bras Endocrinol Metabol*. 2008; 52(4):684–691.
31. Vogelsang H, et al. Bone disease in vitamin D-deficient patients with Crohn's disease. *Dig Dis Sci*. 1989;34(7):1094–1099.
32. Driscoll RH Jr, Meredith SC, Sitrin M, Rosenberg IH. Vitamin D deficiency and bone disease in patients with Crohn's disease. *Gastroenterology*. 1982; 83(6):1252–1258.
33. Harries AD, Brown R, Heatley RV, Williams LA, Woodhead S, Rhodes J. Vitamin D status in Crohn's disease: association with nutrition and disease activity. *Gut*. 1985;26(11):1197–1203.
34. Ulitsky A, et al. Vitamin D deficiency in patients with inflammatory bowel disease: association with disease activity and quality of life. *JPEN J Parenter Enteral Nutr*. 2011;35(3):308–316.
35. Ananthakrishnan AN, et al. Higher predicted vitamin D status is associated with reduced risk of Crohn's disease. *Gastroenterology*. 2012;142(3):482–489.
36. Jostins L, et al. Host-microbe interactions have shaped the genetic architecture of inflammatory bowel disease. *Nature*. 2012;491(7422):119–124.
37. Naderi N, et al. Association of vitamin D receptor gene polymorphisms in Iranian patients with inflammatory bowel disease. *J Gastroenterol Hepatol*. 2008;23(12):1816–1822.
38. Pei FH, et al. Vitamin D receptor gene polymorphism and ulcerative colitis susceptibility in Han Chinese. *J Dig Dis*. 2011;12(2):90–98.
39. Simmons JD, Mullighan C, Welsh KI, Jewell DP. Vitamin D receptor gene polymorphism: association with Crohn's disease susceptibility. *Gut*. 2000; 47(2):211–214.
40. Cantorna MT, Munsick C, Bemiss C, Mahon BD. 1,25-Dihydroxycholecalciferol prevents and ameliorates symptoms of experimental murine inflammatory bowel disease. *J Nutr*. 2000;130(11):2648–2652.
41. Froicu M, Weaver V, Wynn TA, McDowell MA, Welsh JE, Cantorna MT. A crucial role for the vitamin D receptor in experimental inflammatory bowel diseases. *Mol Endocrinol*. 2003;17(12):2386–2392.
42. Kong J, et al. Novel role of the vitamin D receptor in maintaining the integrity of the intestinal mucosal barrier. *Am J Physiol Gastrointest Liver Physiol*. 2008;294(1):G208–G216.
43. Pekow J, et al. Gene signature distinguishes patients with chronic ulcerative colitis harboring remote neoplastic lesions. *Inflamm Bowel Dis*. 2013; 19(3):461–470.
44. Madison BB, Dunbar L, Qiao XT, Braunstein K, Braunstein E, Gumucio DL. Cis elements of the villin gene control expression in restricted domains of the vertical (crypt) and horizontal (duodenum, cecum) axes of the intestine. *J Biol Chem*. 2002; 277(36):33275–33283.
45. Wang Y, et al. Vitamin D receptor signaling in podocytes protects against diabetic nephropathy. *J Am Soc Nephrol*. 2012;23(12):1977–1986.
46. te Velde AA, Verstege MI, Hommes DW. Critical appraisal of the current practice in murine TNBS-induced colitis. *Inflamm Bowel Dis*. 2006; 12(10):995–999.
47. Wirtz S, Neufert C, Weigmann B, Neurath MF.

Chemically induced mouse models of intestinal inflammation. *Nat Protoc*. 2007;2(3):541–546.
48. Okayasu I, Hatakeyama S, Yamada M, Ohkusa T, Inagaki Y, Nakaya R. A novel method in the induction of reliable experimental acute and chronic ulcerative colitis in mice. *Gastroenterology*. 1990;98(3):694–702.
49. Cooper HS, Murthy SN, Shah RS, Sedergran DJ. Clinicopathologic study of dextran sulfate sodium experimental murine colitis. *Lab Invest*. 1993; 69(2):238–249.
50. Ostanin DV, et al. T cell transfer model of chronic colitis: concepts, considerations, and tricks of the trade. *Am J Physiol Gastrointest Liver Physiol*. 2009; 296(2):G135–G146.
51. Powrie F. T cells in inflammatory bowel disease: protective and pathogenic roles. *Immunity*. 1995; 3(2):171–174.
52. Chen Y, et al. 1,25-Dihydroxyvitamin D(3) suppresses inflammation-induced expression of plasminogen activator inhibitor-1 by blocking nuclear factor-kappaB activation. *Arch Biochem Biophys*. 2011; 507(2):241–247.
53. Chen Y, et al. 1,25-Dihydroxyvitamin D promotes negative feedback regulation of Toll-like receptor signaling via targeting microRNA-155-SOCS1 in macrophages. *J Immunol*. 2013;190(7):3687–3695.
54. Sun J, et al. Increased NF-{kappa}B activity in fibroblasts lacking the vitamin D receptor. *Am J Physiol Endocrinol Metab*. 2006;291(2):E315–E322.
55. Chen Y, Zhang J, Ge X, Du J, Deb DK, Li YC. Vitamin D receptor inhibits nuclear factor κB activation by interacting with IκB kinase β protein. *J Biol Chem*. 2013;288(27):19450–19458.
56. Abreu MT, et al. Measurement of vitamin D levels in inflammatory bowel disease patients reveals a subset of Crohn's disease patients with elevated 1,25-dihydroxyvitamin D and low bone mineral density. *Gut*. 2004;53(8):1129–1136.
57. Neurath MF, Fuss I, Kelsall BL, Stuber E, Strober W. Antibodies to interleukin 12 abrogate established experimental colitis in mice. *J Exp Med*. 1995; 182(5):1281–1290.
58. Chen Y, et al. 1,25-Dihydroxyvitamin D promotes negative feedback regulation of TLR signaling via targeting microRNA-155-SOCS1 in macrophages. *J Immunol*. 2013;190(7):3687–3695.
59. Mora JR, Iwata M, von Andrian UH. Vitamin effects on the immune system: vitamins A and D take centre stage. *Nat Rev Immunol*. 2008;8(9):685–698.
60. Hart PH, Gorman S, Finlay-Jones JJ. Modulation of the immune system by UV radiation: more than just the effects of vitamin D? *Nat Rev Immunol*. 2011;11(9):584–596.
61. Zasloff M. Antimicrobial peptides in health and disease. *N Engl J Med*. 2002;347(15):1199–1200.
62. Gombart AF, Borregaard N, Koeffler HP. Human cathelicidin antimicrobial peptide (CAMP) gene is a direct target of the vitamin D receptor and is strongly up-regulated in myeloid cells by 1,25-dihydroxyvitamin D3. *FASEB J*. 2005;19(9):1067–1077.
63. Wang TT, et al. Direct and indirect induction by 1,25-dihydroxyvitamin D3 of the NOD2/CARD15-defensin beta2 innate immune pathway defective in Crohn disease. *J Biol Chem*. 2010; 285(4):2227–2231.
64. Fritz T, Niederreiter L, Adolph T, Blumberg RS, Kaser A. Crohn's disease: NOD2, autophagy and ER stress converge. *Gut*. 2011;60(11):1580–1588.
65. Stappenbeck TS, et al. Crohn disease: a current perspective on genetics, autophagy and immunity. *Autophagy*. 2011;7(4):355–374.
66. Yuk JM, et al. Vitamin D3 induces autophagy in human monocytes/macrophages via cathelicidin. *Cell Host Microbe*. 2009;6(3):231–243.
67. Cooney RM, Warren BF, Altman DG, Abreu MT, Travis SP. Outcome measurement in clinical trials for Ulcerative Colitis: towards standardisation. *Trials*. 2007;8:17.
68. Mary JY, Modigliani R. Development and validation of an endoscopic index of the severity for Crohn's disease: a prospective multicentre study. Groupe d'Etudes Therapeutiques des Affections Inflammatoires du Tube Digestif (GETAID). *Gut*. 1989; 30(7):983–989.
69. Li YC, et al. Targeted ablation of the vitamin D receptor: an animal model of vitamin D-dependent rickets type II with alopecia. *Proc Natl Acad Sci U S A*. 1997;94(18):9831–9835.
70. Butzner JD, Parmar R, Bell CJ, Dalal V. Butyrate enema therapy stimulates mucosal repair in experimental colitis in the rat. *Gut*. 1996;38(4):568–573.
71. Beck PL, et al. Exploring the interplay of barrier function and leukocyte recruitment in intestinal inflammation by targeting fucosyltransferase VII and trefoil factor 3. *Am J Physiol Gastrointest Liver Physiol*. 2010;299(1):G43–G53.
72. Appleyard CB, Wallace JL. Reactivation of hapten-induced colitis and its prevention by anti-inflammatory drugs. *Am J Physiol*. 1995;269(1 pt 1):G119–G125.
73. Park CM, Reid PE, Walker DC, MacPherson BR. A simple, practical "swiss roll" method of preparing tissues for paraffin or methacrylate embedding. *J Microsc*. 1987;145(pt 1):115–120.
74. Hyland NP, Chambers AP, Keenan CM, Pittman QJ, Sharkey KA. Differential adipokine response in genetically predisposed lean and obese rats during inflammation: a role in modulating experimental colitis? *Am J Physiol Gastrointest Liver Physiol*. 2009;297(5):G869–G877.
75. Denning TL, et al. Expression of IL-10 receptors on epithelial cells from the murine small and large intestine. *Int Immunol*. 2000;12(2):133–139.
76. Zhang Z, Zhang Y, Ning G, Deb DK, Kong J, Li YC. Combination therapy with AT1 blocker and vitamin D analog markedly ameliorates diabetic nephropathy: blockade of compensatory renin increase. *Proc Natl Acad Sci U S A*. 2008;105(41):15896–15901.
77. Li YC, Bolt MJG, Cao L-P, Sitrin MD. Effects of vitamin D receptor inactivation on the expression of calbindins and calcium metabolism. *Am J Physiol Endocrinol Metab*. 2001;281(3):E558–E564.
78. Mercurio F, et al. IKK-1 and IKK-2: cytokine-activated IκB kinases essential for NF-κB activation. *Science*. 1997;278(5339):860–866.
79. Yuan W, et al. 1,25-dihydroxyvitamin D3 suppresses renin gene transcription by blocking the activity of the cyclic AMP response element in the renin gene promoter. *J Biol Chem*. 2007;282(41):29821–29830.